

# Nuclear polarization measurements of oriented $^3\text{He}$ gas by "frequency jump" spectrometry\*

R. S. Timsit<sup>†</sup> and J. M. Daniels

Physics Department, University of Toronto, Toronto, Ontario M5S 1A7, Canada

(Received 14 October 1975; in final form, 26 April 1976)

An NMR technique capable of yielding measurements of polarization of highly oriented  $^3\text{He}$  gas without appreciably disturbing the state of nuclear orientation is described. The nuclear polarization is determined through a measurement of dispersive shifts in the frequency of the NMR oscillator as the magnetic field is swept through resonance, rather than from the magnitude of NMR signals.

## I. INTRODUCTION

The polarization of a nuclear spin assembly (e.g., an oriented nuclear target) is most commonly measured by NMR techniques. The nuclear polarization is generally computed either directly from the absolute strength of the NMR induction signal or indirectly by comparing the magnitude of this signal to that generated by some standard sample of known magnetization. Polarization measurements by either method entail at least a partial depolarization of the spin system under investigation. Generally the disturbance is tolerable because the time taken to reestablish the nuclear polarization of nuclei in conventional samples is relatively short. When the spin pumping time is long, however, as is the case in oriented  $^3\text{He}$  gas at high pressure,<sup>1</sup> the depolarization induced by the process of measurement represents a difficulty that must be overcome. It is the purpose of this article to describe an NMR technique capable of measuring the polarization of oriented  $^3\text{He}$  gas without appreciably affecting the state of nuclear orientation. The technique rests on the use of dispersive jumps in the frequency of an NMR oscillator, rather than on the magnitude of induced NMR signals as in adiabatic passage methods, to provide a determination of spin polarization. Although the results reported below were obtained exclusively with polarized  $^3\text{He}$  gas, the natural extension of the method to other spin species should present no special difficulty.

## II. ORIGIN OF THE FREQUENCY JUMP

For the purpose of our discussion it is sufficient to consider the NMR oscillator as consisting of a parallel LC circuit, the inductance of which contains the NMR sample, connected via an untuned high gain amplifier in a positive feedback loop. In analyzing the effects of nuclear resonance absorption on the electrical characteristics of the NMR coil, it is conventionally assumed that the spin assembly behaves as a passive energy-absorbing system. As a general rule, this assumption is valid since the energy dissipated in the NMR sample is small in comparison with the energy available in the tank circuit of the oscillator. The effect of resonant nuclear absorption is thus primarily viewed as

decreasing the effective  $Q$  of the NMR coil. As the external magnetic field is varied to sweep the resonant frequency of the nuclei, the frequency of the oscillator makes small but continuous excursions about the value  $LC^{-1/2}$ . The situation is totally different when a significant fraction of the energy generated by the coil is absorbed by the spin system. Under those conditions the high but not purely resistive loading of the coil by the sample near magnetic resonance not only causes appreciable dispersive shifts in the resonant frequency of the tank circuit but can also bring about sudden frequency jumps.

It is possible to estimate the value of polarization for which frequency instabilities (significant shifts or jumps) will first be observed in our  $^3\text{He}$  NMR samples. Through a conventional analysis of NMR absorption<sup>2</sup> it is possible to show that the maximum change  $\delta V$  in the amplitude  $V$  of the voltage across the tank coil due to nuclear resonance absorption is approximately given by

$$|\delta V/V| \approx Q(h\gamma^2/\Delta\omega)(N/v)P, \quad (1)$$

where  $h$  and  $\gamma$  have their usual significance,  $Q$  is the quality factor of the coil,  $N$  and  $v$  are the number of spins and volume of the coil respectively,  $\Delta\omega$  is the full width at half-height of the absorption line (assumed Lorentzian), and  $P$  is the nuclear polarization of the sample. In our experimental arrangement in which the parameters  $N$ ,  $v$ ,  $Q$  and  $\Delta\omega/2\pi$  have values of  $1.4 \times 10^{21}$  atoms,  $120 \text{ cm}^3$ , 26 and 9.1 Hz, respectively, Eq. (1) reduces to

$$|\delta V/V| \approx 13.7 P. \quad (2)$$

For the conventional analysis to be valid and no significant dispersive frequency shift to appear, the right-hand side of Eq. (2) should be considerably below unity and should certainly not exceed a value of approximately 0.1. Taking this as the value of  $|\delta V/V|$  determining the onset of instabilities in the NMR oscillator frequency, we conclude that a  $^3\text{He}$  polarization in excess of approximately 0.007, i.e., a value considerably smaller than that which can usually be achieved in optically oriented  $^3\text{He}$ , will cause the frequency pulling effects discussed above. This criterion for the onset of

frequency instabilities is very approximately valid in practice. We now proceed with a more exact treatment of the frequency jump phenomenon.

The impedance  $Z(\omega)$  of the unloaded circuit is given by

$$Z(\omega) = |Z(\omega)| \exp[j\theta(\omega)], \quad (3)$$

where  $\theta(\omega)$  is the phase angle and  $Z(\omega)$  is given by

$$Z^{-1}(\omega) = j\omega C + 1/(r + j\omega L),$$

where  $r$  is the coil resistance. When the NMR sample is introduced into the tank coil the inductance is modified and may be written

$$L'(\omega) = L[1 + 4\pi\eta\chi(\omega)], \quad (4)$$

where  $\eta$  is the filling ratio of the sample and  $\chi(\omega)$  stands for the conventional susceptibility of the gas. Writing  $\chi(\omega)$  as  $[\chi'(\omega) - j\chi''(\omega)]$ , the real and imaginary parts of the susceptibility are given by

$$\chi'(\omega) = - (4\pi^2\mu^2/h\Delta\omega)\rho P[(\omega - \omega_R)g(\omega) - (\omega + \omega_R)g(-\omega)] \quad (5)$$

and

$$\chi''(\omega) = (2\pi^2\mu^2/h)\rho P[g(\omega) - g(-\omega)],$$

where  $g(\omega)$  is defined as

$$g(\omega) = (\Delta\omega/2\pi)\{1/[(\omega - \omega_R)^2 + (\Delta\omega/2)^2]\}. \quad (6)$$

Here  $\rho$  and  $\omega_R$  are the gas density and the precession frequency of the spin system, respectively. It is important to note that the function  $g(\omega)$  is *not defined* in terms of the resonant frequency of the coil, which is still unknown. It is expressed instead in terms of the magnetic field  $H$  through  $\omega_R = \gamma H$  and thus determines through Eqs. (5) the extent to which the impedance  $Z(\omega)$  of the circuit is affected at the frequency  $\omega$  by the presence of the precessing spin system. For any setting of the magnetic field, the LC circuit oscillating frequency is determined by the value of  $\omega$  at which the phase angle  $\theta(\omega)$  is zero.

The origin of the frequency instability is best explained diagrammatically by referring to the curves of Fig. 1, which illustrate the changes in the impedance characteristics of the LC circuit as the external magnetic field is swept across the resonance region. These curves were computed from Eqs. (3)–(6) for a nuclear polarization of 5% using the values of  $r$ ,  $L$ ,  $C$ , and  $\eta$  characteristic of our tank circuit, i.e., 3.35  $\Omega$ , 590  $\mu\text{H}$ , 0.078  $\mu\text{F}$ , and 0.338, respectively. The magnitude of the linewidth  $\Delta\omega/2\pi$  was determined from absorption line-shape measurements carried out at low polarizations where dispersive shifts are negligible, and was measured to be 9.1 Hz. Figure 1(a) refers to the impedance characteristics of the tank circuit when the static magnetic field is set far from the resonance region. Assuming that the NMR oscillator amplifier is characterized by zero net phase-shift, we find that oscillations will occur at the frequency  $\omega_0$  (nearly identical with  $LC^{-1/2}$ ) since this frequency corresponds to the zero of the phase-angle curve.

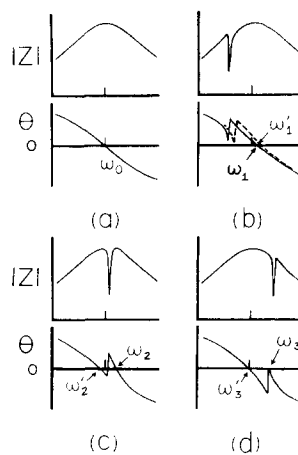


FIG. 1. Frequency response of both the magnitude  $|Z(\omega)|$  and the phase angle  $\theta(\omega)$  of the complex impedance of the LC circuit loaded with the NMR cell, for various settings of the external magnetic field: (a) The field is set far below the resonance value of  $H_0 = \omega_0/\gamma$  and the zero of  $\theta(\omega)$  is nearly equal to  $\omega_0$ ; (b) the field  $H_b$  is set slightly below  $H_0$ , shifting the zero of  $\theta(\omega)$  to  $\omega_1$ ; the sharp dip is centered near  $\omega_R = \gamma H_b$ ; (c) the field  $H_c$  is set slightly above  $H_0$ , causing the phase-angle curve to cross the abscissa three times; the frequencies  $\omega_2$  and  $\omega_2'$  lie respectively to the right and to the left of the center of the dip in  $|Z(\omega)|$  near  $\omega_R = \gamma H_c$ ; (d) the field  $H_d > H_0$  at which the frequency jump ( $\omega_3 - \omega_3'$ ) occurs.

Consider the situation when the external magnetic field  $H_b$  is set below the value  $H_0 = \omega_0/\gamma$  by an increment not exceeding a few NMR absorption linewidths. Under these circumstances the coupling between the precessing nuclei and the coil becomes significant. As shown by the full curves in Fig. 1(b), the function  $|Z(\omega)|$  now displays a prominent absorption dip near  $\omega_0$  at the location of the nuclear precession frequency  $\omega_R$ ; in addition the monotonicity of the phase-angle curve  $\theta(\omega)$  is broken by a distortion also in the vicinity of  $\omega_R$ . We note that the zero of  $\theta(\omega)$  is now no longer coincident with  $\omega_0$  but instead is displaced to the right to the value  $\omega_1 > \omega_0$ . Since this zero determines the instantaneous resonant frequency of the LC circuit the frequency  $\omega_1$  represents the new NMR oscillator operating frequency.

Consider now the effect on the frequency of the NMR oscillator of a small increase in external field strength over the value  $H_b$ . As shown by the dotted curve of Fig. 1(b), this increase causes a further advance of the perturbation ripple of the phase-angle curve to higher frequencies and hence induces an additional positive shift (to  $\omega_1'$ ) in the operating frequency of the oscillator. Thus the NMR oscillator frequency continues its climb. As the field is still further increased the coupling between the NMR sample and the tank circuit eventually becomes such that the  $\theta(\omega)$  curve is characterized by multiple zeros, as illustrated in Fig. 1(c) (corresponding to a field  $H_c$ ). Under these circumstances the determination of the instantaneous oscillator frequency is no longer unambiguous but experimentally it is found that the frequency at all times remains on the high side of  $\omega_R$  during the upward field sweep, i.e., the oscillator is mode-locked at  $\omega_2$  in Fig. 1(c). On the other hand, and as will be clarified below, oscillations occur on the low side of  $\omega_R$  (at  $\omega_2'$ ) when the field traverse is carried out in the opposite direction. The dependence of the frequency on the external field thus possesses hysteresis characteristics.

The concluding sequence of events leading to the frequency jump is as follows. As the external field is further increased a specific field value  $H_d$  is reached wherein the phase-angle curve is characterized by only two zeros as is shown in Fig. 1(d). Under these condi-

tions the tank circuit barely oscillates at the frequency  $\omega_3$ . The slightest increase in the external field will spontaneously force the system to oscillate at  $\omega_3' < \omega_0$  since this now represents the one and only zero of the phase-angle function. The observed negative frequency jump is thus

$$\Delta f = (\omega_3 - \omega_3')/2\pi. \quad (7)$$

The occurrence of the frequency jump is indicative of the fact that the load-induced perturbation of the phase-angle curve is situated wholly below the  $\omega$ -abscissa. In contradistinction to the case illustrated in Fig. 1(b), it thus follows that the unique zero of the  $\theta(\omega)$  function now lies to the left of the  $|Z(\omega)|$ -load dip. This indicates that the oscillator will now remain mode-locked on the low frequency side of the load dip until a new frequency jump condition is reached on lowering the field. This new frequency jump will be positive.

In view of the effect of the external field on the NMR oscillator frequency the question which arises is whether a state of exact resonance between the NMR sample and the rf field is ever attained under any circumstance. An examination of the magnitudes of the fields  $H_b$ ,  $H_c$  and  $H_d$  in Fig. 1 indeed reveals that  $\omega_1 > \gamma H_b$ ,  $\omega_2 > \gamma H_c$  and  $\omega_3 > \gamma H_d$ , indicating that exact magnetic resonance conditions could not have been achieved at intermediate magnetic field settings in this particular situation. Wider considerations do show that this conclusion is general. Extensive computer calculations of the frequency response of the LC tank circuit, spin loaded in a variety of ways, as a function of magnetic field strength indeed indicate that exact resonance between the NMR sample and rf field is impossible so long as frequency jumps do occur.

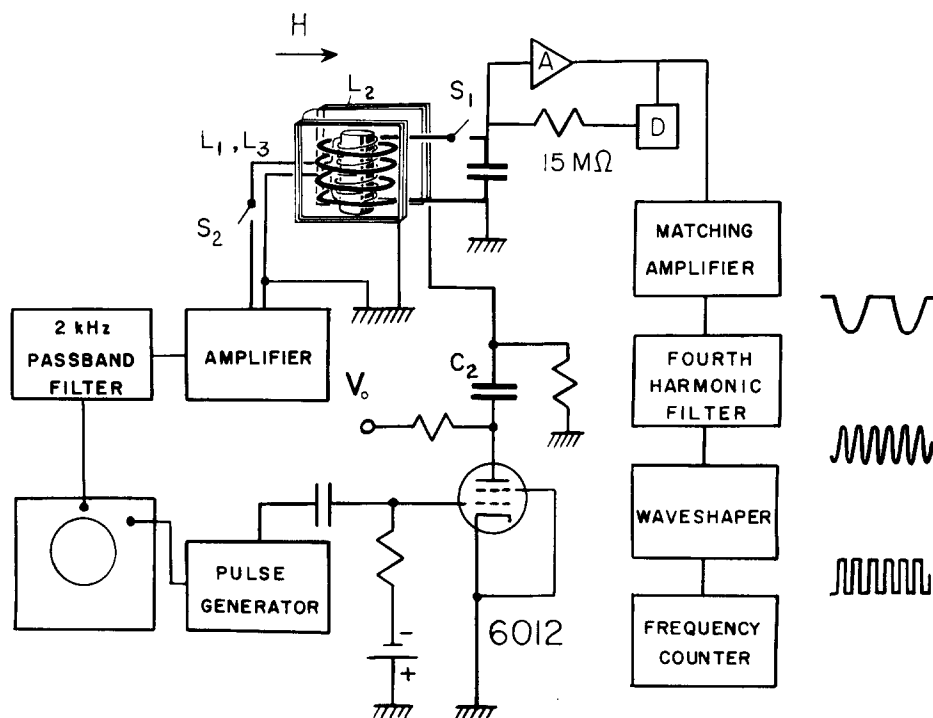
In the following section we shall present experimental evidence to substantiate the arguments put forward above. In addition we shall find it possible to relate the magnitude of the frequency jump  $\Delta f$  to the nuclear polarization  $P$ .

### III. APPARATUS

The magnitude of the frequency jump  $\Delta f$  obtained from the low-level oscillator was related to the nuclear polarization of the  $^3\text{He}$  gas by determining the magnetization of the NMR sample by  $\pi/2$  pulse spectrometry immediately following the measurement of  $\Delta f$ . A block diagram of the apparatus used is shown in Fig. 2. The NMR sample is wrapped with three independent coils shown as  $L_1$ ,  $L_2$ , and  $L_3$ , connected respectively to the tank circuit of the low-level oscillator and to the transmitter and receiver of the  $\pi/2$ -pulse spectrometer. The two NMR spectrometers are kept uncoupled through the judicious use of switches  $S_1$  and  $S_2$ . With  $S_1$  closed and  $S_2$  open the low-level oscillator is operational. With  $S_1$  open and  $S_2$  closed the pulsed NMR spectrometer may be used. Because optical orientation of the  $^3\text{He}$  gas is performed with high-power rf light sources,<sup>3</sup> special care was taken to fit the NMR cell and coils inside a metal can so that they could be operated in a rf shielded environment.

The low-level NMR oscillator is of the type described by Robinson<sup>4</sup> and consists of an LC tank circuit connected to the untuned wide-band amplifier  $A$  whose output is fed into a limiter  $D$ . The limiter produces a half-rectified signal output, independent of the tank circuit voltage, which is fed back through a high-resistance  $R_f$  to the oscillator tank circuit. By making  $R_f$  sufficiently large, the feedback current provided to the

FIG. 2. Block diagram of apparatus used to relate the magnitude of the frequency jump to the  $^3\text{He}$  nuclear polarization.  $A$  and  $D$  are the broad-band amplifier and limiter of the NMR oscillator; coils  $L_1$  and  $L_3$  are connected in series with switches  $S_1$  and  $S_2$ , respectively; the transmitter coil  $L_2$  is placed in series with the discharging capacitor  $C_2$ , itself connected to the switching thyatron tube 6012; the waveforms shown on the right represent the shapes of the signals at the output of each of the three stages preceding the input to the frequency counter.



LC circuit may be maintained both constant irrespective of the impedance of the resonant circuit and as low as is required. Amplifier A consists of five tube stages providing a total gain of  $3 \times 10^5$  over a bandwidth spreading from 1 kHz to approximately 30 MHz. The limiter circuitry closely follows that described by Robinson (also using a 6AK7 tube) and together with a feedback resistor of 15 M $\Omega$  allowed stable oscillations at a tank voltage amplitude of approximately 10  $\mu$ V. As is shown in the Appendix the magnitude of the oscillating tank voltage is sufficiently low to leave the spin assembly essentially undisturbed by one NMR passage. Figure 3(a) shows a typical signal output from the matching amplifier of unity gain connected in parallel with the limiter D. The rectified signal has an amplitude of approximately 3 V and a noise level of about 1/10 of this.

The operating frequency of the NMR oscillator is monitored by measuring the frequency of the fourth harmonic component of the rectified output. This was deemed necessary when it became evident that the amplitude of the fundamental signal was too noisy to provide a steady trigger for the frequency counter. The fourth harmonic filter amplifier used to drive the frequency counter consists simply of two tuned IF stages connected in series; the IF coils are tuned to 93.5 kHz and provide a net passband of approximately 3 kHz. The wave-shaper consists of a straightforward monostable multivibrator producing a rectangular signal clipped at the top and bottom so as to minimize the amount of noise signal getting through to the frequency counter from the NMR oscillator.

The transmitter circuit of the  $\pi/2$  pulse spectrometer consists of a thyratron (No. 6012) connected to a resonant series LC circuit composed of the rectangular coil  $L_2$  and a discharging capacitor  $C_2$  of suitable value. The transmitter delivers a one-half sine wave current pulse generating a peak magnetic field of amplitude  $V_0 F / \omega L_2$ , where  $F$  and  $L_2$  are the number of  $G \cdot A^{-1}$  and inductance of the coil respectively, and  $V_0$  is the charging voltage of the series capacitor. Excellent  $\pi/2$  pulses were obtained with a value of  $V_0$  of 750 V and a pulse length of 3.1  $\mu$ sec ( $L_2 = 14.5 \mu$ H) in a main field of 8.4 G. The transmitter coil  $L_2$  was sufficiently large that the magnetic field produced by the pulse could be considered homogeneous over the NMR sample. The receiver coil  $L_3$  consists of 82 turns of No. 22-gauge copper wire wound on a Lucite mount fitting tightly over the NMR sample. It is connected directly into a high-input-impedance variable gain amplifier which is followed by a narrow passband filter (passband of 2 kHz), peaked at 27 583 Hz. The amplified voltage signal induced in coil  $L_3$  is displayed on the screen of an oscilloscope which is triggered externally by the single-pulse generator used to initiate the current pulse in  $L_2$ . A representative figure for the overall gain of the receiver (including the amplifier and filter) used for the calibration runs was  $10^4$ . The gain was known accurately to approximately 0.2%. Typical examples of induction

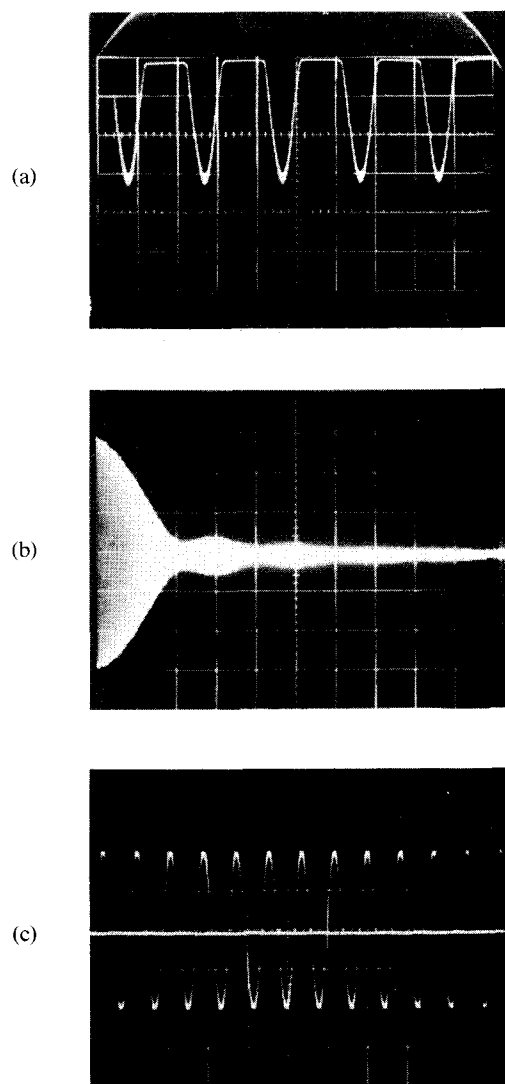


FIG. 3. (a) Signal at output of matching amplifier in Fig. 2. The vertical scale is 1 V/div; (b) free induction decay signal in coil  $L_3$  following a  $\pi/2$  pulse in coil  $L_2$ , the horizontal time base 20 msec/div; the beats are caused by small field inhomogeneities in the sample (as we have verified quantitatively); (c) initial part of signal shown in (b); the horizontal time base is 50  $\mu$ sec/div.

signals displayed on the oscilloscope screen are shown in Figs. 3(b) and (c).

The electromagnet used to provide the static external field has been described in detail in another publication.<sup>5</sup> It produces a maximum field of about 10 G uniform to approximately one part in  $10^3$  over a volume of some 25 liters. The magnet current is stable to 5 parts/million over a period of a few minutes and is monitored by means of a manganin shunt and a digital voltmeter. The power supply for the magnet is swept using a potentiometer driven by a 115-V synchronous motor.

The polarization of the NMR sample is related to the initial amplitude  $V_c$  of the signal induced in pick-up coil  $L_3$  by the expression

$$V_c/G = 2\pi\nu\mu N_0(n\pi a^2)(1 - \alpha)\beta(\rho P), \quad (8)$$

where  $G$  is the overall gain of the amplifying electronics,  $\nu$  is the precession frequency for which the pulse spectrometer is tuned,  $N_0$  is Avogadro's number,  $\rho$  and

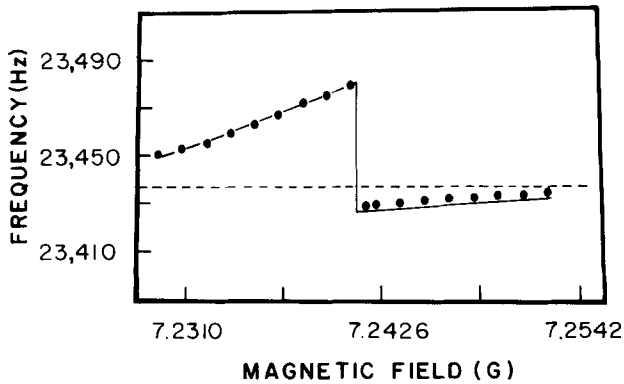


FIG. 4. Variation of NMR oscillator frequency with magnitude of external magnetic field; the dotted horizontal line represents the location of the resonant frequency of the unloaded LC circuit. The solid curve is calculated as explained in the text.

$P$  are the density and polarization of the  $^3\text{He}$  gas, respectively,  $n$  and  $a$  the number of turns and radius of the pick-up coil, respectively, and  $\alpha$  is the demagnetization factor of the sample. The density  $\rho$  is computed from the known temperature and pressure of the gas in the NMR cell.<sup>6</sup> The quantity  $\beta$  is a correction factor which accounts for the presence of magnetic flux in the region bounded by the internal cylindrical wall of the NMR cell and that of the pick-up coil. This flux, which is generated by the magnetized  $^3\text{He}$  sample, runs in opposition to the nuclear magnetization and acts to reduce the amplitude of the signal generated in the pick-up coil by the precessing nuclear magnetization following a  $\pi/2$  pulse. Both the quantities  $\alpha$  and  $\beta$  depend on the geometry of the sample and have to be separately evaluated. The demagnetization factor  $\alpha$  was directly interpolated from Brown's data<sup>7</sup> to have the value 0.208 (for a cell length-to-diameter ratio of 1.73). The factor  $\beta$  was evaluated from the expression

$$\beta = \frac{\sum_i \left\{ \int_{S_i} \mathbf{H}_{\text{in}} \cdot d\mathbf{S}_i + \int_{\sigma_i} \mathbf{H}_{\text{out}} \cdot d\boldsymbol{\sigma}_i \right\}}{\sum_i \int_{S_i} \mathbf{H}_{\text{in}} \cdot d\mathbf{S}_i, \quad i = 1, \dots, n. \quad (9)}$$

Here  $\mathbf{H}_{\text{in}}$  and  $\mathbf{H}_{\text{out}}$  are the fields generated inside the  $^3\text{He}$  sample and between the NMR cell and the pick-up coil, respectively, by the oriented nuclei;  $S_i$  is the inner cross-sectional area of the cell at the location of the  $i$ th turn of the coil, and  $\sigma_i$  is the cross-sectional area of the gap separating the inside cylindrical wall of the cell and the pick-up coil. In the experimental arrangement used, for which the quantity  $a$  and the inner radius of the cell were 2.16 cm and 1.71 cm, respectively, the value of  $\beta$  was calculated to be 0.924, certainly an important correction! Numerical evaluation of Eq. (8) thus leads to

$$V_c/G = 3.86 \times 10^{-3} \rho P, \quad (10)$$

where  $\rho$  is expressed in amagats. We have used Eq. (10) to relate the initial amplitude of the oscilloscope trace to the corresponding  $^3\text{He}$  nuclear polarization.

#### IV. EXPERIMENTAL RESULTS AND DISCUSSION

As mentioned earlier, the essential aim of the experimental work was the establishment of a quantitative relationship between the magnitude of the frequency jump  $\Delta f$  and the absolute nuclear polarization  $P$  of the  $^3\text{He}$  NMR sample. A typical experimental run proceeded as follows (refer to Fig. 2): Compressed  $^3\text{He}$  gas previously optically oriented to a given nuclear polarization was introduced into the NMR cell at a density of approximately 1 amagat (the procedure involved in this step has been described in a separate work)<sup>6</sup>. Switch  $S_1$  was closed and the NMR oscillator frequency measured for a number of magnetic field settings lying both below and above the value of the field for which the frequency jump occurred. Switch  $S_2$  was kept open during this operation to prevent any loading effect of  $L_3$  on  $L_1$ . The switches were then reversed and the magnetic field immediately increased to a value corresponding to a resonant frequency of 27 583 Hz. This does not alter the polarization of the gas but does increase the accuracy to which it may be measured using the pulsed NMR system. A single depolarizing  $\pi/2$  pulse was then applied to  $L_2$  and the nuclear polarization was deduced from the signal induced in  $L_3$  using Eq. (10). This established the correlation between one value of the frequency jump and the nuclear polarization. By repeating this experimental run with gas samples previously optically oriented to different nuclear polarizations the dependence of  $\Delta f$  on  $P$  was established. We now elaborate on the results.

A typical variation of NMR oscillator frequency with magnetic field is shown in Fig. 4. As the field is increased from a low setting through the "resonance" region the oscillator frequency  $\omega$  shifts to values significantly higher than the resonant frequency  $\omega_0/2\pi = 23\,437$  Hz of the unloaded LC tank circuit. At a field strength of 7.2407 G there is a sudden drop in the magnitude of  $\omega/2\pi$  from 23 480 Hz to 23 428 Hz or to a value lying slightly below  $\omega_0/2\pi$ . On further increasing the field the oscillator frequency tends again towards the unloaded circuit value. This oscillator behavior is in accordance with that predicted in Sec. II. Following the  $\pi/2$ -flip measurement of the magnetization, the polarization of the helium sample corresponding to Fig. 4 was deduced to be 0.018. This set of measurements thus establishes that a nuclear polarization of 0.018 at a helium density of 1 amagat produces a jump  $\Delta f$  of 52 Hz in the instantaneous frequency of the NMR oscillator. The more complete experimental dependence of  $\Delta f$  on nuclear polarization, or more precisely on the oriented spin density  $\rho P$ , of the  $^3\text{He}$  gas is shown in Fig. 5. We note that this dependence is relatively strong varying from 23 to 83 Hz for oriented spin densities ranging from 0.005 to 0.03, respectively. Furthermore, this dependence appears linear in the range of polarization densities investigated within the accuracy of the experimental measurements. We estimate that the experimental points of Fig. 5 have a typical error circle no larger than 6%.

It is convenient to have an explicit expression for the curve best fit to the experimental points of Fig. 5. This relation between  $\rho P$  and  $\Delta f$  is linear and is given by

$$\rho P = (1/23)(\Delta f - 10), \quad (11)$$

where  $\rho$ ,  $P$ , and  $\Delta f$  are expressed in amagats, percent, and Hz, respectively. Equation (11) represents the expression sought to deduce  $\rho P$  from a measurement of  $\Delta f$ . The range of validity of this relation will be discussed below. The fact that the calibration curve, as expressed by Eq. (11), does not extend through the origin may be best understood by referring back to Fig. 1. For sufficiently low values of  $\rho P$ , i.e., of the order of 0.1 amagat %, the tank coil of the NMR oscillator LC circuit is negligibly affected by the precessing nuclear magnetization of the  $^3\text{He}$  sample. As a result, the "load spikes" present in the impedance curve [e.g., Fig. 1(b)] are reduced to such negligible magnitudes that the function  $\theta(\omega)$  develops no more than a single zero for any setting of the magnetic field. The abrupt frequency jumps  $\Delta f$  are thus no longer observed for sufficiently low values of  $\rho P$ .

It is possible to compare the experimental data of Figs. 4 and 5 with that expected theoretically on the basis of Eqs. (3)–(6). In computing the dependence of the oscillator frequency on the magnitude of the external field for the conditions corresponding to Fig. 4 the following procedure was adopted: A value for the main magnetic field  $H$  lying well below resonance was selected. The quantity  $\omega_R$  in Eq. (6), corresponding to  $\gamma H$ , was thus defined and the inductance  $L'(\omega)$  of expression (4) evaluated as a function of  $\omega$ . The phase-shift function  $\theta(\omega)$  was then computed from Eq. (3) and its zero(s) determined. Since the traverse direction of the magnetic field was assumed positive, the frequency of the NMR oscillator corresponded to the largest computed zero as explained earlier. The entire procedure was then repeated for successively higher but closely spaced values of  $H$  and the complete spectrum of "largest" zeros of  $\theta(\omega)$ , i.e., the spectrum of the instantaneous oscillator frequencies, as a function of  $H$ , for a polarization density  $\rho P$  of 0.018, was thus tabulated. In these calculations the values assumed for the parameters  $r$ ,  $L$ ,  $C$ ,  $\eta$ , and  $\Delta\omega/2\pi$  were those given in Sec. II. The results are shown by the full curve of Fig. 4. The agreement between the observed and computed data is seen to be excellent. By repeating the above calculations for various values of the  $^3\text{He}$  polarization density it is possible to compute the magnitude of the frequency jump as a function of  $\rho P$ . The results of these calculations are shown by the full curve of Fig. 5. Again the agreement between the observed and theoretical data is excellent. In fact the difference between the experimental best-fit curve given by Eq. (11) and the theoretical curve is indiscernible in the figure over the polarization density range for which Eq. (11) was determined. Indeed the theoretical calculations reveal that Eq. (11) is correct for a value of  $\rho P$  extending at least to 20 amagat %. The theoretical curve

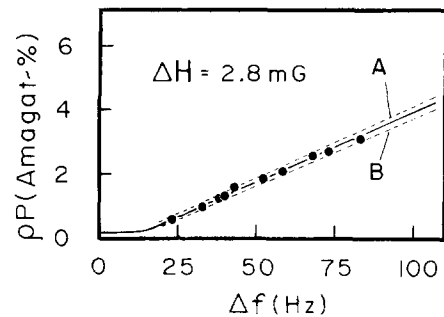


Fig. 5. Dependence of the magnitude of the frequency jump  $\Delta f$  on the oriented spin density  $\rho P$ ; the full curve is calculated for an absorption linewidth of 2.8 mG, the dotted curves A and B are calculated for linewidths of 3.0 and 2.6 mG, respectively.

further shows that, as mentioned above, no frequency jump can be expected to be observed for values of polarization densities smaller than approximately 0.2 amagat %. This is generally consistent with what has been observed experimentally with several  $^3\text{He}$  samples of very low polarization.

The error associated with the theoretical curve of Fig. 5 arises primarily from the uncertainty in the choice of the intrinsic linewidth  $\Delta\omega$  appearing in Eq. (6). In order to illustrate the sensitivity of the computed curve to the choice of linewidth we have computed an additional two curves for linewidths  $\Delta\omega/\gamma$  of 2.6 and 3.0 mG, respectively. These curves are shown as dotted lines in Fig. 5. According to these results it may thus be claimed that the linewidth yielding the best theoretical fit to the experimental data is given approximately by  $2.8 \pm 0.2$  mG. As this is in good agreement with the value of  $3.0 \pm 0.5$  mG determined from NMR absorption profile analyses, we conclude that the agreement between the experimental and theoretical  $\rho P$ -vs- $\Delta f$  curve is excellent within experimental error.

## ACKNOWLEDGMENTS

The authors wish to thank A. K. C. Kiang for assembling much of the electronics used in this work and W. Hilger for providing technical assistance during the course of the experiments. We also wish to thank Professor A. D. May for suggesting several useful modifications to the preliminary draft of this article.

## APPENDIX: EFFECT OF MEASUREMENT OF NUCLEAR RESONANCE ABSORPTION AND FREQUENCY JUMP ON $^3\text{He}$ POLARIZATION

The maximum amount of energy  $E_m$  absorbed during one traverse through resonance in a conventional NMR experiment in which no frequency jumps occur is given approximately by  $W_m(\omega_0/2\pi)[\Delta H/(dH/dt)]$ , where  $W_m$  is the maximum energy dissipated per cycle in the spin system (i.e., at exact resonance),  $dH/dt$  is the magnetic field sweep rate, and  $\Delta H$  is the absorption linewidth in gauss. Using the conventional expression for  $W_m^2$  we find

$$E_m = (\pi V^2 / H_0 \omega_0 L v [1 / (dH / dt)] (2N \mu H_0 P),$$

where  $H_0$  is the external field at resonance,  $L$  is the coil inductance, and the other quantities have already been defined in the text. In our experimental situation the traverse speed is  $6 \times 10^{-5}$  G sec $^{-1}$  and the tank voltage  $V$  is approximately 10  $\mu$ V. The above equation thus reduces to  $7.0 \times 10^{-4}(2N \mu H_0 P)$ . Since the quantity  $2N \mu H_0 P$  represents the energy required to depolarize the entire NMR sample, we conclude that less than 0.07% of the sample polarization is destroyed during a single NMR sweep. In a measurement which involves frequency jumps, the depolarization is much less than this because the nuclei are not swept through resonance, but jump through it.

- \* Work supported in part by the National Research Council of Canada. A brief account of the contents of this article was given at the 1973 meeting of the Canadian Association of Physicists; see R. S. Timsit, "Measurements of the Nuclear Polarization of Highly Oriented  $^3\text{He}$  Gas," *Phys. Can.* **29**, 4, 1973.
- † Present address: Alcan International Ltd. Research Centre, P.O. Box 8400, Kingston, Ontario K7L 4Z4, Canada.
- <sup>1</sup> "Progress Report for the University of Toronto polarized  $^3\text{He}$  Target," Physics Department, University of Toronto (December 1972).
- <sup>2</sup> A. Abragam, *The Principles of Nuclear Magnetism* (Oxford U. P., Oxford, 1962).
- <sup>3</sup> J. M. Daniels, R. S. Timsit, A. D. May, and V. L. S. Yuen, *Can. J. Phys.* **49**, 517 (1971).
- <sup>4</sup> F. N. H. Robinson, *J. Sci. Instrum.* **36**, 481 (1959).
- <sup>5</sup> J. M. Daniels, A. K. C. Kiang, and P. Kirkby, *Can. J. Phys.* **49**, 576 (1971).
- <sup>6</sup> R. S. Timsit, W. Hilger, and J. M. Daniels, *Rev. Sci. Instrum.* **44**, 1722 (1973).
- <sup>7</sup> W. F. Brown, Jr., *Magnetostatic Principles in Ferromagnetism* (North-Holland, Amsterdam, 1962).